

**FIRST LIGHT WITH THE “KERMIT”
NEAR-INFRARED CAMERA¹**

Marshall D. Perrin², James R. Graham, Michael Trumpis

*Astronomy Department, University of California, 601 Campbell Hall, Berkeley, CA 94720,
mperrin@astron.berkeley.edu, jrg@astron.berkeley.edu*

Jeff Kuhn², Kathryn Whitman², Roy Coulter

*Institute for Astronomy, University of Hawaii, 2680 Woodlawn Dr., Honolulu, HI 96822,
kuhn@ifa.hawaii.edu, whitman@ifa.hawaii.edu*

James P. Lloyd

*Department of Astronomy, California Institute for Technology, Pasadena, CA 91125
jpl@astro.caltech.edu*

and

Lewis C. Roberts, Jr.

*AMOS - The Boeing Company, 535 Lipoa Pkwy, Suite 200, Kihei, HI 96753,
lewis.c.roberts@boeing.com*

Abstract

Kermit is an infrared astronomical camera built by the University of Hawaii and the University of California, Berkeley, for high dynamic range observations with the AEOS adaptive optics system, particularly direct imaging surveys for exoplanets. Kermit saw first light at AEOS in April of 2003, and will return in fall 2003 as the science camera for the Lyot Project coronagraph. UH developed the camera optics and mechanics, while UC Berkeley produced the readout electronics and software. Incorporating a state-of-the-art four megapixel Hawaii-2 infrared detector sensitive from 0.8 to 2.5 microns, reflective optics optimized for high dynamic range imaging with low scattered light, and a high-speed 32 channel readout system, Kermit enables infrared astronomical studies with the high-order correction capabilities of the AEOS adaptive optics system. We describe the design and development of Kermit, present data from its first observing run showing the high Strehl ratios achievable at AEOS in the near infrared, and discuss future plans for the camera.

¹Based on observations made at the Maui Space Surveillance System operated by Detachment 15 of the U.S. Air Force Research Laboratory's Directed Energy Directorate.

²Visiting Astronomer, the Maui Space Surveillance System.

1. Introduction

The AEOS adaptive optics system’s 941-element deformable mirror provides higher order wavefront correction than any other astronomical adaptive optics system. It currently produces images with Strehl ratios of typically ~ 0.15 in the *I*-band for objects brighter than 6th magnitude, with Strehl ratios as high as ~ 0.25 observed during upper-quartile seeing conditions [1]. Adaptive optics performance improves substantially as one moves to longer observation wavelengths. The Maréchal approximation for Strehl ratio implies *H*-band performance will have Strehl ratios from 0.60 to 0.90, making AEOS an ideal platform to test key technologies in the emerging field of diffraction-limited coronagraphy. The Lyot Project aims to develop such a coronagraph and with it survey nearby stars for planetary companions and circumstellar disks [2; 3].

The Lyot Coronagraph requires a science camera sensitive at the Near Infrared (NIR, 1-2.5 μm) wavelengths where the sensitivity gain from AO coronagraphy is predicted to be greatest. We developed such a camera to meet the needs of the coronagraph project. This camera, which we named “Kermit” for its green color, is now functional and will be used for observations with the Lyot Coronagraph starting this fall.

In addition, Kermit is capable of being operated in a stand-alone (non-coronagraphic) mode, providing a flexible general purpose NIR imaging capability for AEOS. Kermit achieved first light on the sky in this mode in April 2003 as part of an ongoing multi-wavelength turbulence study [4]. The quality of data obtained, even with poor seeing, demonstrates the potential of NIR observations with the AEOS telescope: images with Strehl ratio as great as 0.83 were observed in *H*-band. We here describe the instrument in detail, present some results from this first observing run, and describe remaining tasks in the development of this instrument.

2. Optical and Mechanical Design

Kermit is built around a Rockwell Hawaii-2 2048 \times 2048 pixel detector as a general purpose, reasonably fast readout, high dynamic range camera for the J, H, and K astronomical bands (1-2.5 μm). For low background applications it must also have reimaging optics that allow for a cold pupil stop within the dewar volume. We chose the unit magnification, telecentric Offner relay [5; 6], which consists of two concentric spherical mirrors with radii of curvature related by $R_1 = 2R_2$. The Offner relay is attractive for its simplicity and freedom from all third-order aberrations. Optical design took place at the University of Hawaii Institute for Astronomy (IfA), with fabrication by IR Labs (Tucson, AZ) and the IfA Scientific Instrument Shop.

The Offner design reimages a field a few centimeters in front of the dewar window onto the detector. Figure 1 shows the Offner relay optical configuration within the dewar. The first element to the left, partially hidden behind the filter wheel, is a wedged fused silica entrance window, which has been antireflection coated from 0.8-2.5 μm . The next element is a seven-position transmissive filter wheel, tilted at 5 degrees to prevent reflective ghosts. The primary concave spherical mirror M1 (focal length 250 mm) forms an image of the telescope pupil onto the secondary mirror, M2. A

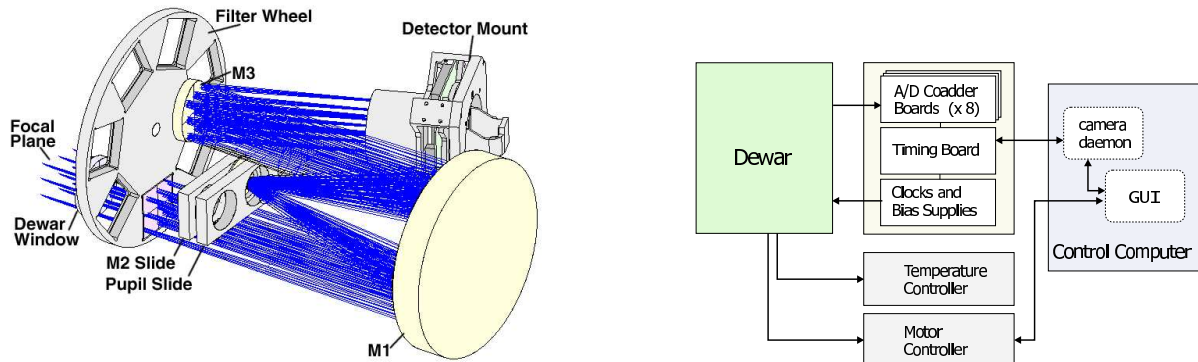


Fig. 1.— **Left:** Kermit optical design and mechanical design. M1 is the concave Offner primary here seen from behind, M2 the convex secondary, and M3 a flat fold-mirror. **Right:** Block diagram of the major components of the Kermit electronics.

slide mechanism allows a variety of cold pupils to be inserted into the beam immediately in front of M2. This 125 mm focal length convex optical element is also mounted on a slide to allow for three secondary mirrors with different coatings. The return beam is focused by the primary mirror and is then folded by a flat mirror, M3, before reaching the detector. Mirrors all use gold coatings. The focal plane array can be translated for focus over a range of about 2 cm along the folded optical axis.

This design is quite robust to alignment errors. For example, decentering M2 by as much as a few mm enlarges the diffraction limited blur circles by less than a pixel width. For M2 decenters in the plane of the off-axis illumination of M1 the design is tolerant to even larger alignment errors. Tilt errors of M2 as large as one degree yield image degradation less than one pixel (assuming no compensating M2 despace or decenter).

A novel feature of this instrument is that the secondary mirror is interchangeable, allowing a fully reflecting IR camera optical design. In this case the gold M2 mirror is replaced by an IR dichroic. This optic reflects at wavelengths shortward of 1.8 microns and transmits to a light stop behind the mirror at longer wavelengths. In this mode the internal filter wheel can be rotated to an open position so that the camera images only shortwave (non-thermal) light. Additional wavelength selection is then possible using warm filters outside of the dewar, including tunable filters which cannot function at cryogenic temperatures.

All four mechanisms (filter wheel, cold Lyot stop slide, M2 slide, and array focus slide) are driven using warm stepper motors from outside of the dewar, using standard IR Labs ferrofluidic couplings and ball-bearing slides. Motor limit and home encoding is provided by mechanical switches, and motor control is by a Galil 2200 series controller.

The dewar is cooled using a CTI model 1040 Helium cryocooler, which provides sufficient cooling power to hold the dewar work plate at 50 K. Dewar cool-down takes approximately 10 hours. The detector fanout board is clamped thermally, but not electrically, to the cold work plate via a flexible copper strap. A temperature sensor and heater mounted directly on the strap provide temperature regulation by a Lakeshore 331-S temperature controller. In practice the system is able to hold the temperature there very precisely at 75.000 K, with fluctuations less than the measurement uncertainty of ± 0.005 K.

3. Electronics and Software

The readout electronics and control software for Kermit were developed at UC Berkeley, building upon the widely used readout electronics system available from Astronomical Research Cameras, Inc., and software developed for the IRCAL camera used with the Lick Observatory Adaptive Optics system [7]. A block diagram indicating the major subsystems is given in figure 1.

3.1. Detector

The detector is a 2048×2048 Hawaii-2 array from Rockwell Scientific Corp. This is the largest currently available HgCdTe infrared focal plane array (FPA), with a size of $37 \text{ mm} \times 37 \text{ mm}$ and a pixel pitch of 18 microns. It is sensitive from 0.8 to 2.5 microns with roughly 60% quantum efficiency across that range. Full well depth is 10^5 electrons, with dark current < 0.03 electrons/second at 78 K and read noise < 10 electrons using correlated double sampling. The Hawaii-2 FPA was originally developed by Rockwell for the AEOS Spectrograph project, as described by [8].

The detector is provided by Rockwell in a ceramic carrier designed to mate with a commercially available 21×21 pin Zero Insertion Force (ZIF) socket. The ZIF socket itself is mounted on a fanout circuit board developed at the Institute for Astronomy adapted from that used in the AEOS IR Spectrograph [9]. Ribbon cables connect the fanout board to the pass-through sockets in the dewar wall, from which shielded coaxial cables connect to the readout electronics rack.

3.2. Readout Electronics

The readout electronics for Kermit is a 32-channel Generation II system supplied by Astronomical Research Cameras (ARC) of San Diego, CA [10]. Our configuration features an ARC Gen II timing board, clock and bias driver board, and eight four-channel A/D converter and coadder boards, along with the standard power regulation board and power supply.

The 32 output channels from the detector are connected directly to two-stage amplifiers on the eight A/D converter boards using low-noise Analog Devices AD829 op-amps, and then digitized by ADS931 16-bit ADCs with a conversion time of $1 \mu\text{s}$. The digital output is stored into 32-bit \times 1 Megaword RAM buffers directly on the coadder boards, allowing a maximum readout rate of 32 megapixels/second, or 8 Hz full frame rate.

Certain modifications were needed to the Gen II electronics in order to drive the Hawaii-2 array successfully. The fast clock signals to the Hawaii-2 array (referred to as CLK1, CLK2, CLKB1, and CLKB2 in the standard detector pinout labeling) require rise time < 100 ns, necessitating the replacement on the timing board of the standard AD829 op amps with the faster AD811 (slew rate > 2500 V/s, settling time < 65 ns for a 5V step). Note that CLK1 and CLKB2, and also CLK2 and CLKB1, must be identical signals, and each pair is driven from a single AD811 op-amp output. The detector gate voltage is 2.5V and the reset voltage is 0.5V.

Secondly, the eight A/D converter boards required several modifications. The Hawaii-2 pixel outputs act as current sinks so a pull-up resistor must be supplied. We provided this with a 10 k Ω resistor to +5V at the inputs to the first-stage amplifiers on the A/D boards. The resulting voltage swing is roughly between 3.5 V (zero counts) and 3 V (saturation): only half a volt for the entire range of the detector. By changing resistor values appropriately, we set the second stage inverting amplifier to have a gain of 10. With the first stage amplifier with gain 2, this results in a total gain of 20. Appropriate analog offsets were applied to center the signal in the -10V to 0V input range of the analog to digital converter chip.

Note that we are currently operating the A/D boards in singled-ended rather than differential mode. This is because the high 20x gain made it impractical to difference a 3V signal against ground. Future development of the electronics could potentially add a pixel-level reference signal output to the fanout board, suitable for differential measurement.

3.3. DSP Software

Three layers of control software exist between the camera hardware and the user. The readout electronics are controlled by nine Motorola 56002 digital signal processors (DSPs), one on each A/D board and a master controller on the timing board, which is responsible for producing the readout waveforms. The DSP software used is a heavily modified version of the stock version 1.7 DSP software from ARC. The modifications include support for flexible subarraying, fast readout into the coadder buffer memory, and variable numbers of CDS reads and resets, in addition to the basic waveform changes needed for the Hawaii-2 array.

Two readout speeds are supported: 4 μ s/pixel and 2 μ s/pixel, with the default 4 μ s. Each input channel is a 128 \times 1024 region of the detector (128 pixels in the fast clock direction, 1024 rows in the slow clock direction). Using the 4 μ s pixel time, it therefore takes 524 ms to clock out a full frame. Faster frame rates are available by reading out only a subarray, down to 16 ms for a 64 \times 64 pixel readout. The subarray position is moderately flexible, though complications of detector quadrant and channel geometry currently prevent fully arbitrary placement. The user may select any of the 8 coadder boards for subarray readout and may supply an offset into the array to begin the readout.

Three readout modes are available: Single read, correlated double sampling (CDS), and a CDS mode in which both the initial and final read frames are saved to disk for later subtraction. In all of these modes, any number of multiple reads may be obtained, with the results summed in

hardware before readout. However, due to the long minimum readout time (524 ms full-frame) the camera has so far been operated mostly using only a single pair of CDS reads. Between exposures, the chip is continually reset to prevent the buildup of charge on the detector if a bright source is left there.

The link between the electronics rack and the control computer is provided by a 50 MHz fiber optic link to a PCI card. This link is capable of transferring only 1.5 megapixels/second (using 32 bits/pixel), or about 5.5 seconds to transfer a full-frame single CDS readout. To prevent this from presenting a bottleneck in the readout, many readouts may be coadded together directly in the electronics rack on the A/D cards, and only after the desired number of frames have been obtained is the resulting sum frame transferred to disk.

3.4. Control software and GUI

On the control computer, a daemon written in C interfaces with the readout electronics, including managing the fiber optic link, setting camera parameters, and writing data to disk. The third software layer is a graphical user interface (GUI) written in TCL/Tk, which provides a top-level interface for controlling the camera, including access to all camera settings, motor control, and support for scripting. The camera daemon and GUI communicate via TCP sockets using the Traffic message passing library developed at Lick Observatory [11].

The data acquisition software provides a facility for reference bias subtraction during image readout. A library of dark frames taken with various parameters is maintained, and if the current readout configuration matches one of the extant bias frames, the appropriate frame is subtracted from the image before it is saved to disk. While this does not in general substitute for dark subtraction in data reduction, it is highly successful in suppressing the static bias pattern and bad pixels for the purposes of quick-look image display. The software also maintains a list of all exposures taken during a session in the form of a palette of readout configurations. This enables the operator to easily switch between several configurations throughout a night's observations. The user interface can then automatically generate from this exposure palette a script to automate the acquisition of calibration darks. Images are written to disk in standard FITS format. External 250 GB Firewire hard drives are used for backup and data transfer. The ds9 tool from SAO [12] is used for image display, while the GUI also incorporates an interface to IDL and IDL scripts can be used for quick-look image manipulation.

4. Initial Performance

We were able to commission Kermit during the April 2003 observing run for the AO Turbulence Project. See [4] for a description of the experiment setup in Coude Room 6 of the AEOS 3.6 m telescope at the Maui Space Surveillance System. For this initial run, we operated using an engineering-grade FPA. This device had one good quadrant and three quadrants with degraded or no functionality. The following discussion refers entirely to data taken using the good quadrant.

Table 1: Predicted and Measured AEOS NIR Performance

Band	λ (μm)	Diffraction FWHM (mas)	Measured FWHM (mas)	Predicted Strehl Ratio ^a	Measured Strehl Ratio
<i>J</i>	1.25	71.0	80-142	0.53	0.11-0.45
<i>H</i>	1.65	93.6	93-145	0.69	0.36-0.83
<i>K</i>	2.20	125.0	137-165 ^b	0.81	0.40-?? ^b

^aPredicted Strehl ratios calculated by scaling the observed *I*-band Strehl ratio 0.25 using the Maréchal approximation $S = \exp(-(\sigma/\lambda)^2)$, with σ the RMS wavefront error and λ the wavelength.

^bDue to a lack of narrow-band K filters, sources brighter than $V \sim 6$ saturated the detector in the minimum readout time. Therefore we were only able to accurately measure K band Strehl ratio and FWHM for fainter stars.

We expect to have replaced this device with our science-grade detector before the next observing campaign. The optical set up for this observing run provided a plate scale of 0.021 mas/pixel.

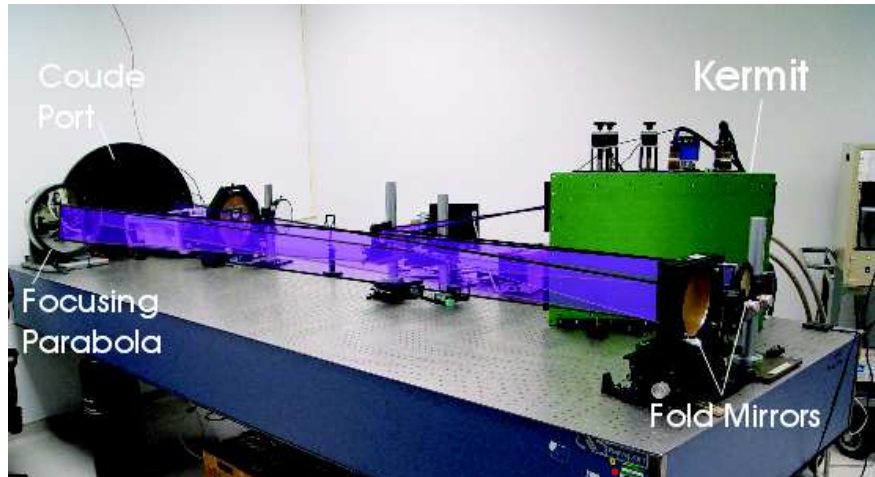


Fig. 2.— The experiment setup in Experiment Room 6 of the AEOS telescope, with the optical path highlighted. Kermit is the large green box at right.

We note that hardware coaddition requires very low residual tip-tilt and tracking errors in order to retain good image quality. The AEOS Coronagraph includes a fast tip-tilt system expected to remove image motion to less than a milliarcsecond, so this is not expected to pose a problem. For the observations in April, residual tip-tilt motion was large enough that we took single exposures rather than coadding in hardware, so that we could register the images before coadding in software.

Conditions during this run were challenging due to weather; we observed only four nights out of fourteen. The on-site seeing monitor was broken except for one of those nights preventing thorough calibration of conditions. For the single night we do have measurements for, seeing was poor, with the mean Fried length at 550 nm equal to 7.5 cm, and at times as low as 3 cm. Further

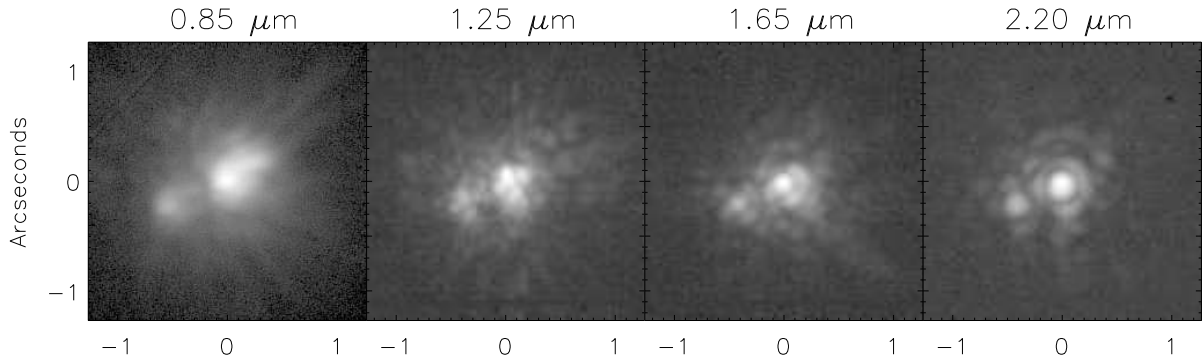


Fig. 3.— The binary star McA 38, with separation $0.5'' = 2.4 \mu\text{rad}$. The figures show how AO correction improves with wavelength. The three right hand images were taken with Kermit, while the left-hand image ($0.85 \mu\text{m}$) was taken with a visible CCD, and is provided for comparison only. All four images are log-stretched single 0.25s exposures, taken within 10 minutes of one another on 2003 April 18.

difficulties arose from internal turbulence in the light pipe and Coude room and vibration of the helium cryocooler cold head.

We are currently in the process of reducing the data, and present here only a subset of our expected eventual results. We obtained data on seven binary pairs and six single stars, taking several dozen frames in each of the J, H, and K bands for most targets. For each observation, we calculated the Strehl ratio by normalizing a theoretical PSF to match stellar photometry and taking the ratio of peak pixels. The relevant code has been tested and found to produce accurate PSFs for well sampled images such as these. We also measured the full-width at half-maximum for each image. For the 512×512 subarray used, the minimum exposure time was 0.25s. We used narrow-band filters to obtain unsaturated images of very bright stars at 1300 nm and 1600 nm, but lacked any narrow K-band filters and so were able to measure Strehl ratio and FWHM only at the faint end of the magnitude range. We will obtain the needed narrow K band filters before our next observing run.

Table 1 presents predicted and observed AEOS performance in the NIR. The observed Strehl ratio increases with wavelength as expected. In general, wavefront correction seemed better for brighter sources, but our small sample size prevents any definitive statement. The best few *H*-band images for a first magnitude star have Strehl ratios just over 0.8, with more typical values in the range 0.6-0.7. This implies a K band performance of around 0.9 for bright sources; we measured a K band Strehl ratio of 0.45 for a $V=7.5$ source. While these results are from a very limited data set taken under conditions of poor and variable seeing, we believe they demonstrate the potential of NIR imaging to take advantage of the AEOS adaptive optics system.

5. Future Work

While apart from the weather, our commissioning effort was largely successful, there remain a few outstanding issues. Foremost among these is that our readout electronics remain sensitive to electromagnetic interference to an untraced ground loop, resulting in greatly increased noise in our images (~ 200 e- RMS). However, the noise pickup is nearly identical for all 32 readout channels, so by taking a median of all channels, we can obtain the noise signal and subtract it from the data. This procedure has proven highly effective, for most images reducing image noise to 20-30 e- RMS. There is also some crosstalk between adjacent detector channels which may be mostly removed by the same process. Work to reduce the effects of interference is currently ongoing.

Secondly, the helium cryocooler used to chill the dewar introduces unwanted vibrations to the optical table, resulting in degraded image quality while the compressor is running. We are considering various options for reducing this vibration. A workaround is to temporarily shut of the compressor while images are being acquired and reactivate it afterwards, but this is not a long-term solution.

There are currently two planned future observing campaigns that will use Kermit: additional observations for the AO Turbulence Project [4], and the Lyot Project stellar companion and disks survey [3]. In addition, potential upgrades to the camera to add capabilities for polarimetry or integral field spectroscopy are under consideration. We believe that near infrared observations on AEOS have the potential for strong scientific return; AEOS provides higher order wavefront correction than any other current astronomical adaptive optics system, and thus offers a unique capability for high Strehl ratio observations and on-the-sky development of diffraction limited coronagraphy.

6. Acknowledgments

The development of this instrument would not have been possible without the contribution of many individuals. We're grateful to Pierre Baudoz for his help with the Kermit optics and mechanical design work, and we thank Klaus Hodapp for his help and assistance with the Hawaii-2 detector. Ev Irwin provided invaluable advice and assistance on detector clocking and readout. Electronics technicians Paul Uemura and Freddie Retuta at UH and Calvin Cheng at UCB contributed greatly to the hardware development. Jill Kajikawa-Kent persevered against many obstacles to get the hardware shipped to AEOS. We would like to thank the staff of the Maui Space Surveillance System for their assistance throughout this project, particularly Wendy Pratt and Peter Figgis who saved the day with a last-minute 220V power line installation.

The US Air Force provided on-site support and research funds for this project, jointly sponsored with the National Science Foundation, under grant number NSF AST-0088316. Additional support for the IfA activities were provided by NSF award AST-0123390. This work has also been supported by the National Science Foundation Science and Technology Center for Adaptive Optics, managed by the University of California at Santa Cruz under cooperative agreement AST-9876783. Telescope time and additional support was provided by the Air Force Office of Scientific Research through

AFRL/DE (Contract Number F29601-00-D-0204). M. Perrin is supported by a NASA Michelson Graduate Fellowship, under contract to the Jet Propulsion Laboratory (JPL) funded by NASA.

REFERENCES

1. Roberts, L. C. and Neyman, C. R. *PASP*, Vol. 114, 1260–1266, 2002.
2. Lloyd, J. P., Graham, J. R., Kalas, P., Oppenheimer, B. R., Sivaramakrishnan, A., Makidon, R. B., Macintosh, B. A., Max, C. E., Baudoz, P., Kuhn, J. R. and Potter, D. *Proc. SPIE Vol. 4490, p. 290-297, Multifrequency Electronic/Photonic Devices and Systems for Dual-Use Applications*, Andrew R. Pirich; Paul L. Repak; Paul S. Idell; Stanley R. Czyzak; Eds., 290–297. 2001.
3. Oppenheimer, B. R., Digby, A. P., Newburgh, N., Brenner, D., Shara, M., Sivaramakrishnan, A., Makidon, R. B., Soummer, R., Roberts, L. C., Graham, J. R., Kalas, P., Perrin, M. D., Kuhn, J. and Whitman, K. *This volume*. 2003.
4. Roberts, L. C., Bradford, L. W., Turner, N. C., ten Brummelaar, T. A., Perrin, M. D., Graham, J. R., Whitman, K., Kuhn, J. and Oppenheimer, B. R. *This volume*. 2003.
5. Offner, A. *Opt. Eng.*, Vol. 14, 150, 1975.
6. Graham, J. R. and Treffers, R. R. *PASP*, Vol. 113, 607–621, 2001.
7. Lloyd, J. P., Liu, M. C., Macintosh, B. A., Sevenson, S. A., Deich, W. T. and Graham, J. R. *Proc. SPIE Vol. 4008, p. 814-821, Optical and IR Telescope Instrumentation and Detectors*, Masanori Iye; Alan F. Moorwood; Eds., Vol. 4008, 814–821. 2000.
8. Thornton, R. J., Kuhn, J. R., Hodapp, K., Stockton, A. N., Luppino, G. A., Waterson, M., Maberry, M., Yamada, H., Irwin, E. M. and Fletcher, K. *Instrument Design and Performance for Optical/Infrared Ground-based Telescopes. Edited by Iye, Masanori; Moorwood, Alan F. M. Proceedings of the SPIE, Volume 4841, pp. 1115-1126 (2003).*, 1115–1126. 2003.
9. Whitman, K., Kuhn, J. R., Waterson, M. and Thornton, R. J. *This volume*. 2003.
10. Leach, R. W. and Low, F. J. *Proc. SPIE Vol. 4008, p. 337-343, Optical and IR Telescope Instrumentation and Detectors*, Masanori Iye; Alan F. Moorwood; Eds., 337–343. 2000.
11. Kibrick, R. I., Stover, R. J. and Conrad, A. R. *ASP Conf. Ser. 52: Astronomical Data Analysis Software and Systems II*, 277–+. 1993.
12. Joye, W. A. and Mandel, E. *ASP Conf. Ser. 295: Astronomical Data Analysis Software and Systems XII*, 489–+. 2003.